Physical infrastructure interdependency and regional resilience index after the 2011 Tohoku Earthquake in Japan

Gian Paolo Cimellaro[1,*,†], Daniele Solari[1] and Michel Bruneau[2]

[1]*Department of Structural, Geotechnical and Building Engineering (DISEG), Politecnico di Torino, 10129 Turin, Italy*
[2]*Department of Civil, Structural & Environmental Engineering, University at Buffalo, 130 Ketter Hall, Buffalo, NY 14260, U.S.A.*

SUMMARY

A resilience index is used to quantify preventive measures, emergency measures, and restoration measures of complex systems, such as physical infrastructures, when they are subjected to natural disasters like earthquakes, hurricanes, floods, etc. Interdependencies among these systems can generate cascading failures or amplification effects, which can also affect the restoration measures right after an extreme event and generate a reduction of the resilience index. In this article, a method is proposed to evaluate the physical infrastructure resilience of a region affected by a disaster considering infrastructure interdependency. It is illustrated using available restoration curves from the March 11 2011 Tohoku Earthquake in Japan. The weights assigned to each infrastructure, which are used to determine resilience, are evaluated using the degree of interdependency indices which are obtain by time series analysis. Results show that the weight coefficients thus obtained do not influence the resilience index significantly; however, the methodology proposed is unbiased from subjective judgment and is able to identify the critical lifelines. Furthermore, the results of the case study presented here suggest that to obtain meaningful estimation of the weight coefficients, it is necessary to consider the period range between two perturbations (e.g., main shock and aftershock). Future infrastructure disruption data (from this and other earthquakes) would be needed to generalize this finding that will allow also to quantify the changes in the restoration curves caused by the magnitude and distance of the shocks from the epicenter, as well as the intrinsic properties of the physical infrastructures. Copyright © 2014 John Wiley & Sons, Ltd.

1. INTRODUCTION

In recent years, the scientific community has become increasingly interested in lifelines interdependencies and resilience evaluation [1, 2] and recent literature includes several papers addressing the evaluation of interdependency indices for infrastructures [3]. These works published in the last decade are all using the taxonomy of lifeline interdependencies, which is given in the fundamental work by Rinaldi *et al.* [4]. Paton and Johnston [5] have provided numerical quantification of the dependencies among different infrastructures, by using an empirical approach in which the degree of dependency among different infrastructures is the function of the strength of the dependency (high, medium, and low dependence). Bigger *et al.* [6] have collected different interdependent lifeline information associated with the 2004 hurricane season in Florida. Delamare *et al.* [7] have studied the potential effect of interdependencies that may occur between the telecommunication and the electrical network, and they have proposed a model that describes the behavior of these interdependent systems. More recently, Kakderi *et al.* [8] have summarized the available methodologies and models for the vulnerability and

---

*Correspondence to: G. P. Cimellaro, Department of Structural, Geotechnical and Building Engineering (DISEG), Politecnico di Torino, 10129 Turin, Italy.
†E-mail: gianpaolo.cimellaro@polito.it

risk assessment of systems of systems. In their work, they summarized and illustrated definitions of the interaction of complex dependencies available in literature. The classification schemes of dependencies were reviewed, and the available methods for the simulation of interdependencies were summarized and classified in five categories. Furthermore, the main characteristics, advantages and limitations of each category of interdependency were also reported. Alternatively, Kongar et al. [9] provided a review of the literature using a matrix approach and used it to describe gaps in knowledge. Based on this review, Kongar et al. proposed a methodological framework for the assessment of infrastructure vulnerability accounting for interdependencies.

Kjølle et al. [10] have used contingency analysis (power flow), reliability analysis of power systems, and cascade diagrams for investigating interdependencies. Poljansek et al. [11] have studied the seismic vulnerability of the European gas and electricity transmission networks from a topological point of view; network interdependency was evaluated using the strength of coupling of the interconnections, together with the seismic response.

Recently, Dueñas-Osorio and Kwasinski [12] have proposed an approach based on post-analysis of restoration curves. The interdependency index between infrastructures was calculated by an empirical equation that depends on the maximum positive value of the cross-correlation function (CCF) of the two data series.

Here, a method is proposed to evaluate the resilience of a region affected by a disaster considering infrastructure interdependency. The resilience index of every infrastructure in the region is combined with others by weight coefficients, which are calculated starting from a modified version of the interdependence index proposed by Dueñas-Osorio and Kwasinski [12] using CCF. A new method to evaluate the interdependency index is proposed and compared with other methods available in literature. The regional resilience index is evaluated taking in account weights coefficients evaluated for every region and infrastructure considered in the analysis. Finally, a method for the treatment of restoration curves is proposed for the case when aftershocks are included in the restoration curves. The method is described using the restoration curves [13] of the physical infrastructures of the 12 regions in Japan, which were affected by March 11 2011 Tohoku Earthquake.

2. RESTORATION CURVES OF PHYSICAL INFRASTRUCTURES AFTER THE 2011 TOHOKU EARTHQUAKE

The proposed method for the evaluation of the interdependency index and the weights coefficients necessary to evaluate the regional resilience index is based on the evaluation of the CCF for different restoration curves. In this paper, the restoration curves used for the analysis are the time series recorded during the March 11 2011 Tohoku Earthquake [13], in the 12 nearby Japanese prefectures of Miyagi, Ibaraki, Fukushima, Yamagata, Akita, Ibaraki, Tochigi, Aomori, Chiba, Gunma, Saitama, and Kanagawa (listed here by increasing distance from the epicenter). The functionality $Q(t)$ in the y-axis of Figure 1 is defined as the restoration ratio between the number of households without service and the total number of households. In particular, in Figure 1 are shown the restoration curves for three different types of lifelines (power delivery, water supply, and city gas delivery) for Miyagi, Iwate, Fukushima, Ibaraki, Aomori, and Saitama. For Yamagata, Akita, Tochigi, and Gunma, only data on power delivery and water supply are available, whereas for the Chiba and Kanagawa prefecture, only restoration curves for the power delivery and city gas delivery are available. Figure 1 also shows the effects on the restoration curves of two main aftershocks, which occurred on April 7th ($M = 7.2$) and on April 11 ($M = 7.0$), on the different infrastructures and regions, respectively. The first aftershock reduced the serviceability in the regions located near the epicenter of the main shock, whereas the second aftershock reduced the serviceability of lifelines in the Fukushima prefecture only. City gas delivery was not influenced by the two aftershocks in any region.

3. EVALUATION OF INTERDEPENDENCY INDEX

To calculate the CCF functions of the different restoration curves, the time series must be at least weakly stationary [14]. To minimize the effects of nonstationary data and to obtain meaningful
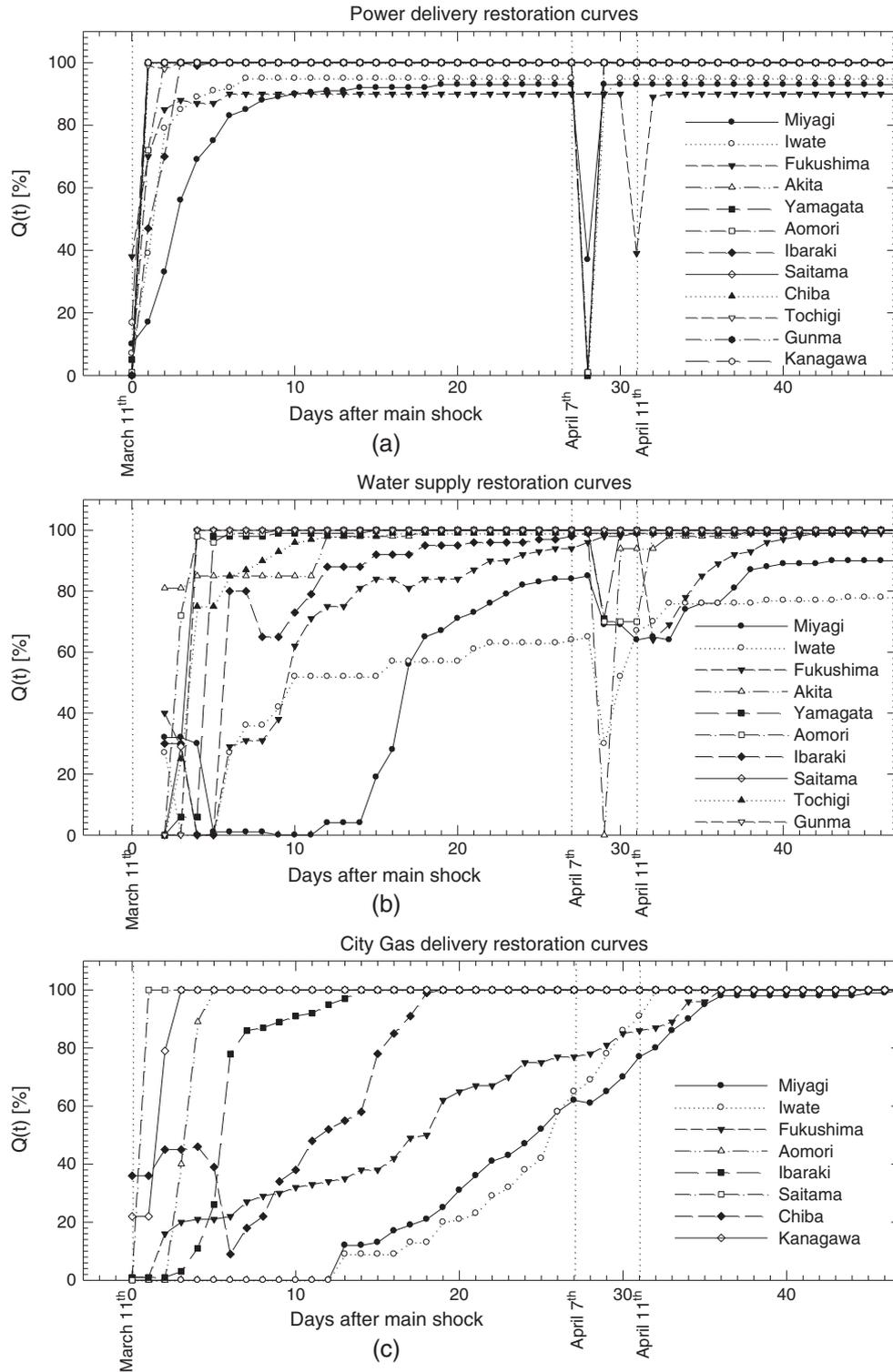
Figure 1. Restoration curves for different Japan prefectures after the 2011-03-11 $Mw = 9.0$ earthquake for three infrastructures: (a) power delivery, (b) water supply, (c) city gas delivery – (Adapted from [13]).

statistical analyses, the time series data have been logarithmically transformed and second-differenced (Figure 2(a)). This transformation stabilizes the variability, and the mean value, which remains constant through time, while the auto-covariance values decay rapidly and only depend on the time-difference
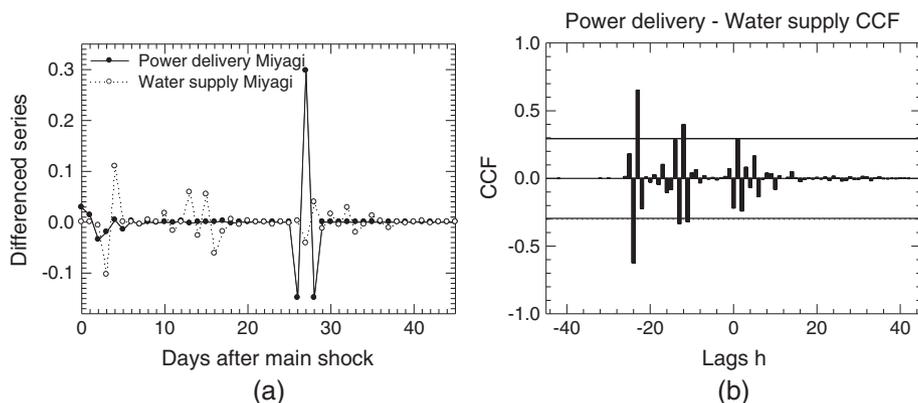
Figure 2. Miyagi region data: (a) power delivery and water supply restoration curves logarithmically transformed and second differenced; (b) cross-correlation function of power delivery, and Water supply versus lags h.

$h = t_1 - t_2$ between the data series, where t_1 and t_2 are arbitrary points in time [14]. An example of the results of the transformation, about power delivery and water supply for the Miyagi region is shown in Figure 2 (a). After the logarithmical transformation and the second-differenced of the data series, it is possible to evaluate the *CCF* functions ($\rho_{i,j}(h)$) for different combinations of the restoration curves.

Figure 2(b) shows an example of *CCF* function between *power delivery* and *water supply* for the Miyagi region. The *x*-axis is the *lag*, analytically defined as a fixed time displacement, which corresponds to the number of periods $k > 0$, that a variable occurring at time $t + k$ lags behind to predict the variable occurring at time t. Four different approaches and equations for the evaluation of the interdependency index $S_{i,j}$ among different infrastructures are proposed (Eqs (2)–(5)) and compared with the results of Equation (1), which has been proposed by Dueñas-Osorio and Kwasinski [12]

$$S_{i,j} = \begin{cases} \dfrac{\rho_{i,j}^+(h)}{1 + \sqrt{|h|}} \times \text{sgn}(h) & when \ h \neq 0 \\ \rho_{i,j}^+(h) & when \ h = 0 \end{cases} \tag{1}$$

where $p_{i,j}^+(h)$ corresponds to the maximum positive *CCF* value, which occurs at the peak lag time value h with absolute value $|h|$, and the sign function (*sgn*) is used to keep track of the dominant system. The ith system leads [lags] the restoration of the jth system when $S_{i,j}$ is positive [negative] [12]. The four proposed alternative equations are

$$S_{i,j} = \begin{cases} \dfrac{\rho_{i,j}^+(h)}{h} & when \ h \neq 0 \\ \rho_{i,j}^+(h) & when \ h = 0 \end{cases} \tag{2}$$

$$S_{i,j} = \frac{1}{N} \sum_{k=1}^{N} \left(\begin{cases} \dfrac{\rho(h_k)}{1 + \sqrt{|h_k|}} \times \text{sgn}(h_k) & when \ \rho(h_k) \geqslant \rho_{tr} \ and \ h_k \neq 0 \\ \rho(h_k) & when \ \rho(h_k) \geqslant \rho_{tr} \ and \ h_k = 0 \end{cases} \right) \tag{3}$$

$$S_{i,j} = \frac{1}{N} \sum_{k=1}^{N} \left(\begin{cases} \dfrac{\rho(h_k)}{h_k} & when \ \rho(h_k) \geqslant \rho_{tr} \ and \ h_k \neq 0 \\ \rho(h_k) & when \ \rho(h_k) \geqslant \rho_{tr} \ and \ h_k = 0 \end{cases} \right) \tag{4}$$

$$S_{i,j} = |A_{i,j}|^{\frac{1}{N}} \cdot \text{sgn}(A_{i,j}) \tag{5}$$

where

$$A_{i,j} = \frac{1}{N} \sum_{k=1}^{N} \left(\begin{cases} \frac{\rho(h_k)}{\sqrt{|h_k|}} \times \text{sgn}(h_k) & when \ \rho(h_k) \geqslant \rho_{tr} \ and \ h_k \neq 0 \\ \rho(h_k) & when \ \rho(h_k) \geqslant \rho_{tr} \ and \ h_k = 0 \end{cases} \right) \tag{6}$$

where $\rho_{i,j}^{+}(h)$ corresponds to the maximum positive *CCF* value, which occurs at the peak lag time value h; $\rho(h_k)$ corresponds to the *CCF* values, which occur at lag time h_k; ρ_{tr} is the value of the positive threshold of statistical significance (the threshold is shown in Figure 2 with the two horizontal solid lines); and N corresponds to the number of *CCF* values that exceed the upper bound of statistical significance. The *n*-infrastructure restoration curves are analyzed, and the results are organized in an $n \times n$ matrix where every element ranges between -1 and 1. Positive values of this index show that the ith infrastructure (row) leads the restoration process of the jth infrastructure (column), while negative value of the index shows that the ith infrastructure (row) lags behind the restoration process of the jth infrastructure (column). The magnitude of the dependence is given by the absolute value of the index; when it is close to 1, the dependency is high, while when it is close to 0 the dependency is weak (zero value indicates absence of dependency).

The results for the March 11 2011 Tohoku Earthquake are shown in Table I, while it is shown in Figure 3 the comparison of the different interdependency indices $S_{i,j}$ evaluated with the different equations for the regions of Miyagi and Iwate, respectively. Equation (5) generally gives the highest values of the interdependency index, while the other equations have lower values of $S_{i,j}$. Equations (3) and (4) have the lowest values of the interdependency index, because the $S_{i,j}$ index are evaluated from the average of the values of the *CCF* function, which exceed the positive threshold of statistical significance. From Table I, it is observed that the interdependency index relative to the power delivery evaluated with the different equations using the restoration curves of 47 days, often has negative value, which has no physical meaning. This behavior is well highlighted, also in Figure 3 where the interdependency index resulting from all the different equations taken into consideration are reported. All equations used for the evaluation of the $S_{i,j}$ index give results that are consistently of the same sign, but differences are observed in the absolute values.

4. EVALUATION OF THE WEIGHT COEFFICIENTS OF THE INFRASTRUCTURES

The weights coefficients, w_i, for the different infrastructures, which are necessary to assess the regional resilience, are calculated with Equation (7). The matrix $S_{i,j}$ is a square matrix in which the terms on the diagonal are always equal to 1, whereas the terms outside the diagonal can range from -1 to $+1$. Positive values indicate that the lifeline in the row 'leads' the lifeline in the column. The weight coefficients are calculated using the positive values of the interdependency matrices ($S_{i,j}$) corresponding to different lifelines. First, all the positive terms, per row, are added. Second, the weight coefficients are calculated as the ratio between the sum of the positive values in one row, and the sum of all positive terms in the matrix $S_{i,j}$, namely

$$w_i = \frac{\sigma_i}{\sum_i \sigma_i} \tag{7}$$

where σ_i is the sum of the positive values of the ith row of the interdependence matrix $S_{i,j}$, given by

$$\sigma_i = \sum_j S_{i,j} \quad when \ S_{i,j} > 0 \tag{8}$$

The physical meaning of the weight coefficients can be explained with an example by assuming that the infrastructures are independent. In this special case, the S matrix is an identity matrix; therefore, the weight coefficients evaluated with Equation (7) will be all identical. Equal weight coefficients in this

Table I. Comparison of different interdependency indices from different equations ($T_{LC} = 47$ days).

Region		S_{ij} Eq. (1) [12]	S_{ij} Eq. (2)	S_{ij} Eq. (3)	S_{ij} Eq. (4)	S_{ij} Eq. (5)
Miyagi	Power - water	−0.11	−0.10	−0.03	−0.03	−0.35
	Power - gas	−0.15	−0.15	−0.05	−0.05	−0.19
	Water - gas	0.10	0.03	0.04	0.00	0.31
Iwate	Power - water	0.33	0.07	0.66	0.21	0.55
	Power - gas	−0.10	−0.13	−0.03	−0.08	−0.56
	Water - gas	−0.10	−0.04	−0.08	−0.03	−0.38
Fukushima	Power - water	0.22	0.04	0.44	0.14	0.47
	Power - gas	−0.11	−0.10	−0.02	−0.03	−0.35
	Water - gas	−0.15	−0.15	−0.11	−0.11	−0.23
Yamagata	Power - water	−0.13	0.02	−0.03	0.16	0.31
Akita	Power - water	0.46	0.46	0.93	0.93	0.93
Ibaraki	Power - water	0.14	0.14	0.09	0.09	0.20
	Power - gas	0.19	0.16	0.12	0.12	0.49
	Water - gas	0.87	0.87	0.87	0.87	0.87
Tochigi	Power - water	0.29	0.29	0.26	0.26	0.45
Aomori	Power - water	−0.13	−0.13	−0.03	−0.03	−0.15
	Power - gas	−0.11	−0.11	−0.03	−0.03	−0.13
	Water - gas	0.72	0.72	0.72	0.72	0.72
Chiba	Power - gas	0.15	0.15	0.11	0.11	0.23
Gunma	Power - water	0.26	0.26	0.23	0.23	0.40
Saitama	Power - water	0.29	0.29	0.27	0.27	0.46
	Power - gas	1.00	1.00	1.00	1.00	1.00
	Water - gas	−0.29	−0.29	−0.27	−0.27	−0.46
Kanagawa	Power - gas	0.28	0.28	0.55	0.55	0.55
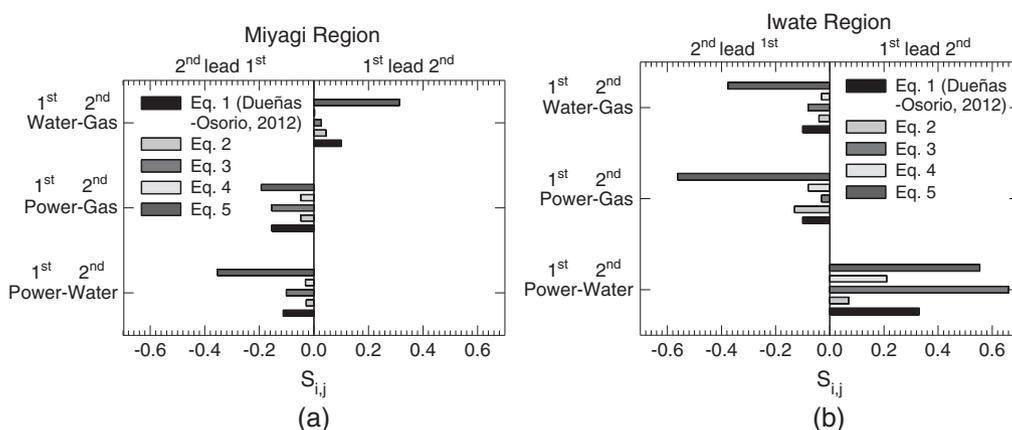
Figure 3. Comparison of different interdependency index proposed for (a) Miyagi and (b) Iwate regions.

particular condition have physical meaning because in this case no infrastructure is leading another one, so no one can be considered more important than the other ones. The different weight coefficients were evaluated using Equations (1)–(5) for the 12 Japanese prefectures affected by the

2011 earthquake and for the three lifelines considered earlier. All the results are shown in Table II, and part of these results are shown in Figure 4 for Miyagi and Iwate prefectures.

5. EVALUATION OF THE REGIONAL RESILIENCE INDEX

Resilience is defined as 'a normalized function indicating capability to sustain a level of functionality or performance for a given building, bridge, lifeline, networks, or community over a period of time T_{LC} (life cycle, life span, etc.)' [1]. Analytically, the resilience index of each infrastructure is given by the following equation [2, 15, 16]:

$$R_i = \int_0^{T_c} \left(\frac{Q_i(t)}{T_c} \right) dt \tag{9}$$

Table II. Weight coefficients for the computation of Regional Resilience.

| | | $S_{i,j}$ | $S_{i,j}$ | $S_{i,j}$ | $S_{i,j}$ | $S_{i,j}$ | |
		Eq. (1) [12]	Eq. (2)	Eq. (3)	Eq. (4)	Eq. (5)	Same weight
Miyagi	Power	0.30	0.32	0.30	0.32	0.26	0.33
	Water	0.36	0.34	0.34	0.34	0.43	0.33
	City gas	0.34	0.34	0.35	0.34	0.31	0.33
Iwate	Power	0.38	0.44	0.42	0.46	0.37	0.33
	Water	0.28	0.27	0.39	0.38	0.24	0.33
	City gas	0.34	0.29	0.19	0.17	0.39	0.33
Fukushima	Power	0.35	0.40	0.40	0.44	0.39	0.33
	Water	0.29	0.28	0.38	0.38	0.27	0.33
	City gas	0.36	0.32	0.22	0.18	0.34	0.33
Yamagata	Power	0.47	0.49	0.75	0.78	0.65	0.50
	Water	0.53	0.51	0.25	0.22	0.35	0.50
Akita	Power	0.59	0.66	0.59	0.66	0.66	0.50
	Water	0.41	0.34	0.41	0.34	0.34	0.50
Ibaraki	Power	0.26	0.24	0.15	0.13	0.27	0.33
	Water	0.37	0.38	0.43	0.44	0.36	0.33
	City gas	0.37	0.38	0.43	0.44	0.36	0.33
Tochigi	Power	0.56	0.56	0.56	0.56	0.59	0.50
	Water	0.44	0.44	0.44	0.44	0.41	0.50
Aomori	Power	0.21	0.22	0.21	0.22	0.21	0.33
	Water	0.40	0.39	0.40	0.39	0.40	0.33
	City gas	0.39	0.39	0.39	0.39	0.39	0.33
Chiba	Power	0.54	0.53	0.54	0.53	0.55	0.50
	City gas	0.46	0.47	0.46	0.47	0.45	0.50
Gunma	Power	0.56	0.55	0.56	0.55	0.58	0.50
	Water	0.44	0.45	0.44	0.45	0.42	0.50
Saitama	Power	0.41	0.41	0.41	0.41	0.42	0.33
	Water	0.18	0.18	0.18	0.18	0.17	0.33
	City gas	0.41	0.41	0.41	0.41	0.42	0.33
Kanagawa	Power	0.56	0.61	0.56	0.61	0.61	0.50
	City Gas	0.44	0.39	0.44	0.39	0.39	0.50
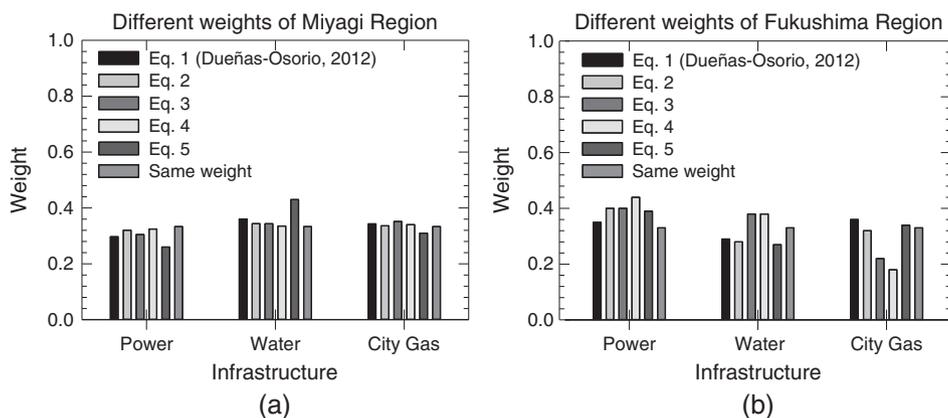
Figure 4. Comparison of different weights coefficients for (a) Miyagi region and for (b) Fukushima region for the three different infrastructures.

where R_i is the value of resilience of the ith infrastructure, $Q_i(t)$ is the functionality of the ith infrastructure at time t, T_c is the control period that is taken in this case to be 47 days (i.e., the length of available records for the March 11 2011 Tohoku Earthquake). Once the weight coefficients are known, the regional resilience index is evaluated, multiplying the resilience of each lifeline by the corresponding weight coefficient (i.e., the one corresponding to the row on which is situated the lifeline in the matrix $S_{i,j}$) and adding the results obtained inside all regions. The regional resilience R is evaluated with Equation (10) using the weights of the different infrastructures calculated with Equation (7).

$$R = \sum_i (R_i \times w_i) \qquad (10)$$

Results are shown in Table III and in Figure 5 for different weights of infrastructure's resilience.

Results in Figure 5 confirm that the major damage occurred in the regions near the epicenter of the main shock (as intuitively expected).

Discrepancies in this trend are observed only for the prefectures facing the Pacific coast (Miyagi, Iwate, Fukushima, Ibaraki, and Aomori) where the tsunami caused relevant damage (lower values of the resilience index), as well as areas far from the epicenter (Chiba and Kanagawa). For example, Chiba suffered more damage than Tochigi even if Chiba is more distant from the epicenter of the earthquake than Tochigi. This is because Chiba is on the Pacific coast while Tochigi is an interior region. Note that resilience in this context should be considered as a response parameter and not as an intrinsic property of the community; therefore, higher values of resilience in a region far from the epicenter, such as Kanagawa, does not necessarily mean that the community itself is resilient to

Table III. Regional resilience index evaluated with different weights (47 days).

Region	Eq. (1) [12]	Eq. (2)	Eq. (3)	Eq. (4)	Eq. (5)	Same weight
Miyagi	0.61	0.62	0.62	0.62	0.61	0.63
Iwate	0.67	0.69	0.69	0.70	0.66	0.65
Fukushima	0.75	0.78	0.77	0.79	0.76	0.76
Yamagata	0.92	0.94	0.92	0.94	0.94	0.92
Akita	0.95	0.95	0.95	0.95	0.95	0.94
Ibaraki	0.88	0.87	0.88	0.87	0.88	0.89
Tochigi	0.94	0.94	0.94	0.94	0.94	0.94
Aomori	0.97	0.97	0.97	0.97	0.92	0.96
Chiba	0.90	0.90	0.89	0.89	0.90	0.89
Gunma	0.95	0.95	0.95	0.95	0.95	0.95
Saitama	0.93	0.93	0.93	0.93	0.97	0.93
Kanagawa	0.97	0.97	0.98	0.98	0.98	0.97
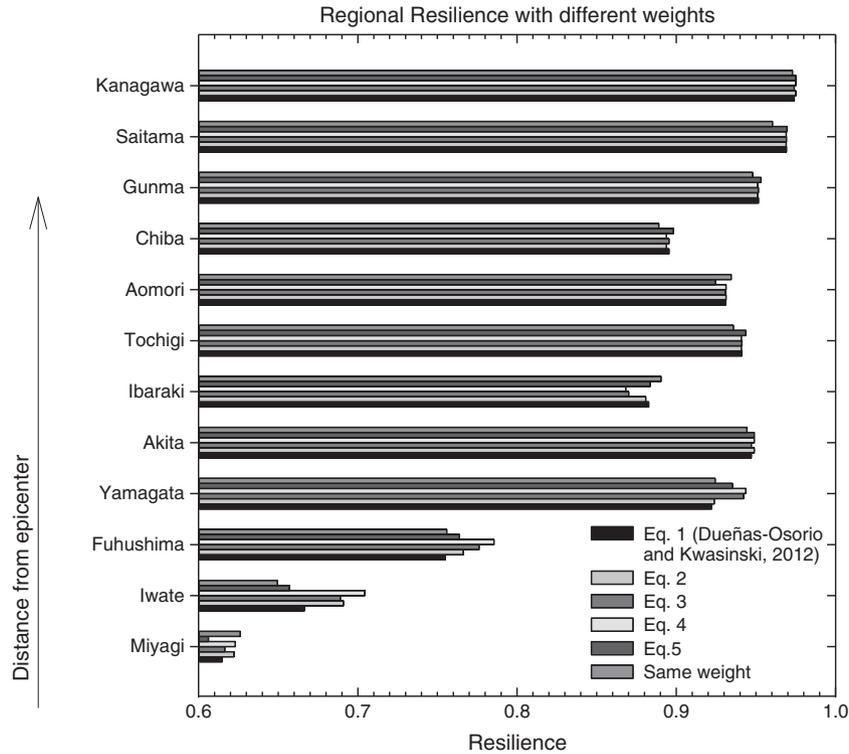
Figure 5. Regional resilience calculated using different methods to calculate weight coefficients starting from the resilience index of every infrastructure.

earthquakes that would occur closer. To translate these results into community resilience, another parameter independent from the earthquake input (or normalizing results in terms of local level of ground shaking) should be taken in account, which is beyond the scope of this paper. Figure 6 shows the standard deviation of the regional resilience index ordered by region according to distance from the epicenter. The values of standard deviation are observed to be higher near the epicenter and progressively decreasing in regions farther from the epicenter. As such, results in Figures 5 and 6 show that the type of approach taken to calculate the weight coefficients does not significantly influence the values of the resilience index for regions far from the epicenter.
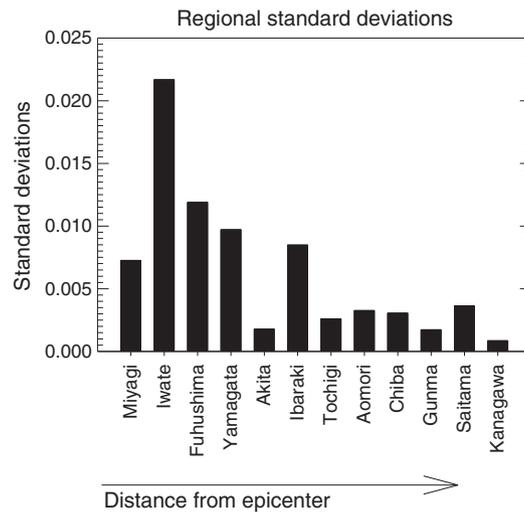
Figure 6. Standard deviation of regional resilience.

6. DISCUSSION ON THE EVALUATION OF THE INTERDEPENDENCY INDICES

The regional resilience index defined in Equation (10) depends on the weight factors (Eq. (7)), which themselves depend on the interdependency indices ($S_{i,j}$). Therefore, a proper methodology to evaluate $S_{i,j}$ is necessary to evaluate resilience. By comparing the interdependency indices proposed in Section 3, it can be observed that Equations (1), (3), and (5) have the denominator term proportional to $\sqrt{|h|}$ that has the effect of amplifying the interdependency index, compared to Equations (2) and (4) that have the denominator term proportional to h (Figure 3). In fact, Equations (1), (3), and (5) give more weight to the lags, which are more distant from lag 0, with respect to Equations (2) and (4). Therefore, if the *CCF* function has one peak only to lag ± 1 (typical for power delivery *CCF* functions), Equations (1) and (3) give a value of $S_{i,j}$, which is roughly half the one obtained using Equations (2), (4), and (5). Equations (1) and (2) consider only the peak positive value of the *CCF* function in their formulation, neglecting the corresponding threshold of statistical significance. Instead Equations (3)–(5) consider only the positive values of the *CCF* function above the respective threshold. According to the authors, the approach followed by Equations (3)–(5) is statistically meaningful, because all peak positive values below the statistical threshold do not have any statistical significance. Therefore, the following observations focus on results obtained from the last three equations.

Equation (3) gives values of $S_{i,j}$ that are lower with respect to the ones obtained using Equations (4) and (5) (because of the form of the denominator described earlier) when the *CCF* functions have only one peak to lag ± 1, which is usually the case for the power delivery *CCF* functions. In fact, after the main shock, the power delivery network suffers a rapid drop of functionality before the other infrastructures, as shown in Figure 1. However, the electric network is also the first lifeline that is repaired after a disaster, because other infrastructures depend on it. These considerations provide good reasons to disregard Equation (3). Because of the structure of the denominator, Equation (4) is less sensitive to the values of the *CCF* far from lag 0 and, in general, gives lower values of the interdependency index with respect to the other equations, as shown in Figure 3. In fact, Equation (4), by averaging the values of the *CCF* functions above the positive threshold, provide lower values of the interdependency index, especially when the *CCF* functions have one of these values that is small, which is usually the case when it is distant from lag 0. Because of this lesser sensitivity in those cases, Equation (4) is less desirable. Equation (5) provides values of $S_{i,j}$ higher with respect to Equation (1), when there is more than one value of the *CCF* function above the positive threshold of statistical significance. Furthermore, Equation (5) is the only one that provides meaningful results, because as shown in Figure 3(b), Equation (5) provides the highest $S_{i,j}$ value for power delivery and lowest values (maximum negative values of $S_{i,j}$) for other infrastructures dependent on this (which is consistent with engineering judgment). Therefore, based on the aforementioned considerations, Equation (5) is retained as the recommended approach for the evaluation of the interdependency indices $S_{i,j}$. Therefore, to investigate robustness of the formulation, sensitivity analysis has been conducted on Equation (5) with different hypothetical CCF functions shapes (Figure 7), and the results are compared with the Equation (1) proposed by Dueñas-Osorio and Kwasinski [12]. Figure 7(a) shows a *CCF* function with a constant value less than 1 (0.8) with the threshold value assumed equal to 0.5, while Figure 7(b) shows the response of Equations (1) and (5) as a function of the number of *CCF* values over the threshold taken into account for the calculation of $S_{i,j}$. It is observed that the two equations give the same result if one considers only the first value at lag 0 over the threshold. However, when increasing the number of *CCF* values taken into account, Equation (5) gives a value of $S_{i,j}$ higher than would be achieved using Equation (1). It is also observed that the difference between the two functions increases when increasing the values of the *CCF* function above the threshold taken into consideration in the calculation. In fact, Equation (5) produces an increment of the interdependency index when there is more than one value of the *CCF* function above the threshold of statistical significance.

For example, Figure 7(c) shows a *CCF* function, which starts from lag 0 with a value of 0.8 and linearly decreases until the value of 0 for a lag of 10. The threshold is also equal to 0.5 in this case. For comparison, Figure 7(d) shows the response obtained by Equations (1) and (5) as function of the number of *CCF* values over the threshold taken into account for the calculation of $S_{i,j}$. Again, if one considers only the first value at lag 0 over the threshold, the two equations give the same result.
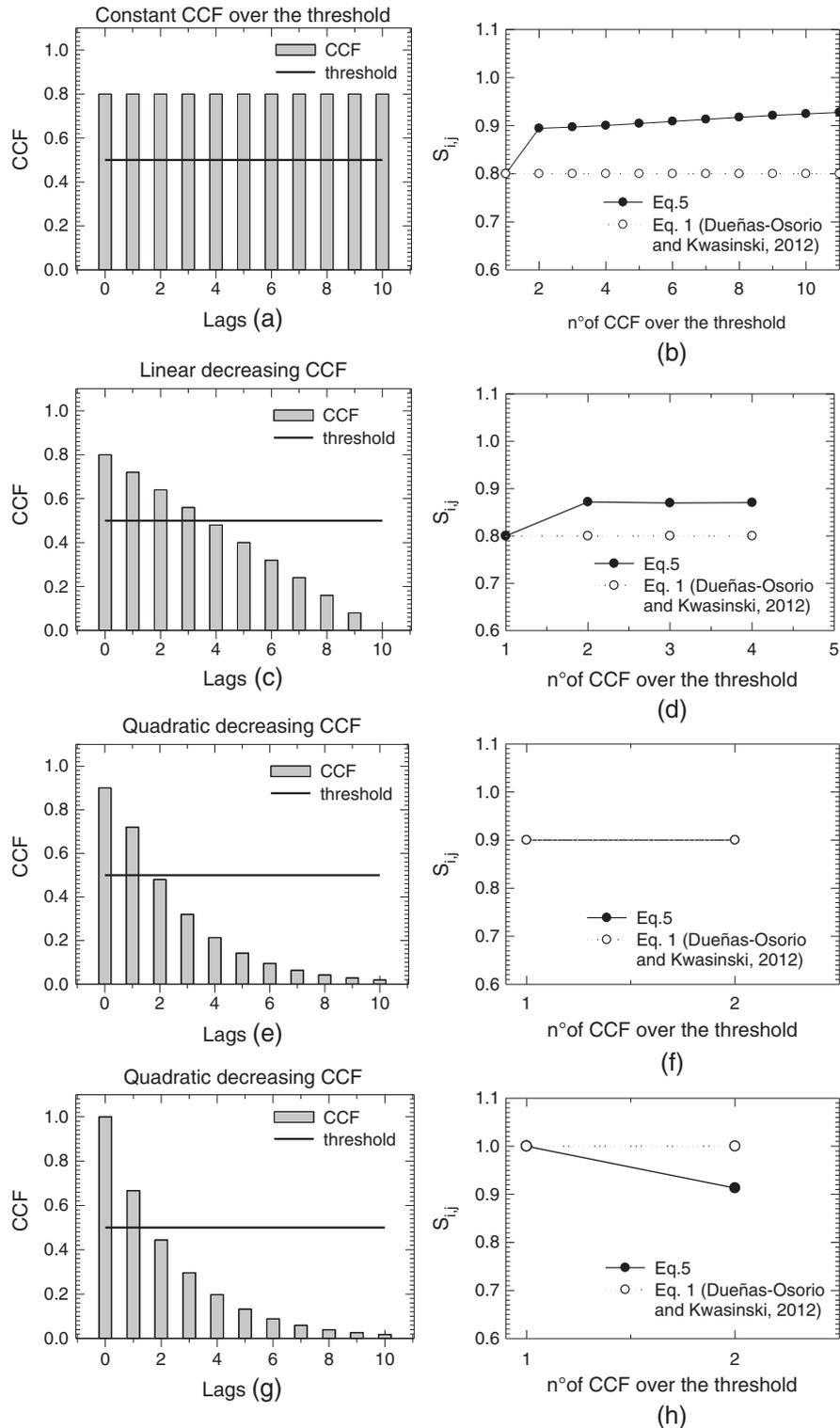
Figure 7. Comparison of the interdependency index between Equations (1) and (5) with quadratic decreasing *CCF* values.

When increasing the number of *CCF* values taken into account, Equation (5) gives $S_{i,j}$ values higher with respect to Equation (1), but the difference between the two functions remains constant; in particular, the difference between the results of Equations (1) and (5) is less with respect to the case

shown in Figure 7(b). Figure 7(f) shows a boundary behavior of Equation (5), which gives the same results as Equation (1) regardless the number of *CCF* values (shown in Figure 7(e)) considered in Equation (5) for the computation of $S_{i,j}$. This behavior appears every time the ratio between the value of the *CCF* function at lag 1 and the value of the *CCF* function at lag 0 is equal to a certain value, which is a function of the value that assumes the *CCF* function at lag 0.

Figure 8 plots the ratio of the 2nd CCF value/1st CCF value versus the 1st CCF value, and compares Equation (1) and (5) by identifying two regions of solutions, namely *Region 1* (where Equation (5) gives a lower $S_{i,j}$ values with respect to Equation (1), as shown in Figures 7(g)–(h)) and *Region 2* (where Equation (5) gives a higher $S_{i,j}$ values with respect to Equation (1)). In particular, the curved line in this figure corresponds to the case when Equation (5) gives the same result of Equation (1), which corresponds to the case shown in Figure 7(e)–(f).

Furthermore, it is observed from this figure that when the first value of the *CCF* function at lag 0 ranges between 0 and 0.5, Equation (5) gives higher values of $S_{i,j}$, regardless the *CCF* function value at lag 1. The sensitivity analysis of the $S_{i,j}$ index evaluated with Equation (5) has been performed to identify the interval of significance, as well as the advantages and limitations of the proposed equation. In fact, in *Region 1*, an increment of the $S_{i,j}$ index using Equation (5) appears when more than one value of the *CCF* function exceeds the threshold of statistical significance (Figure 7), while when the $S_{i,j}$ index appears in *Region 2* (Figure 8), Equation (5) underestimates the $S_{i,j}$ index with respect to Equation (1). Finally, Figure 9 shows the comparison of Equations (1) and (5) for a real
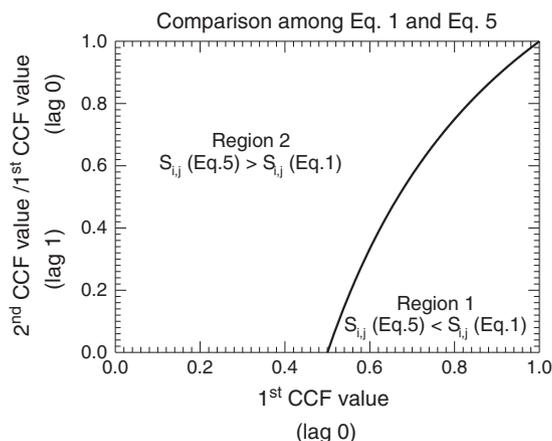
Figure 8. Comparison of cross-correlation function (*CCF*) values between Equation (1) proposed by Duenas-Osorio and Kwasinski [12]) and Equation (5).
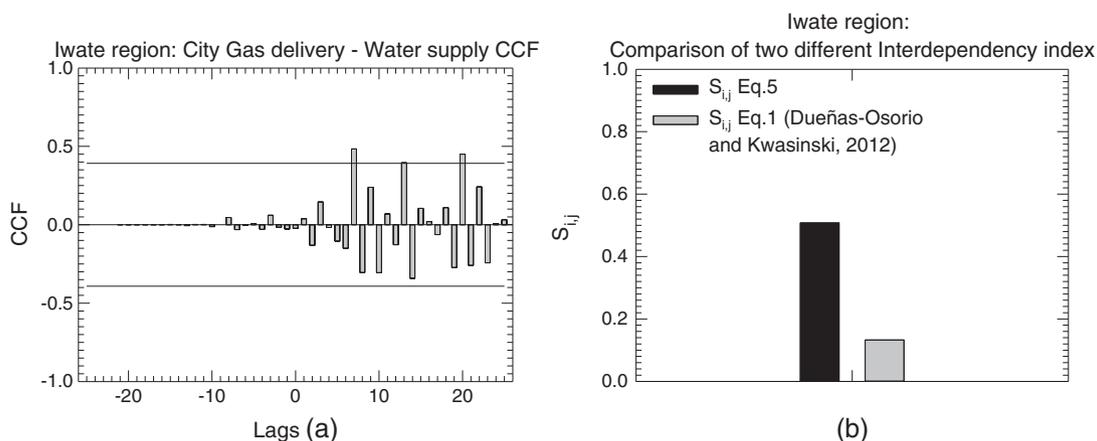
Figure 9. Comparison of interdependency index for city gas delivery and water supply in Iwate region using Equations (1) and (5).

CCF function resulting from the cross-correlation of the restoration curves recorded after the March 11 2011 Tohoku Earthquake [13], relating city gas delivery and water supply for the prefecture of Iwate in Japan. In this real case where more than one value of the *CCF* function exceeds the threshold for statistical significance, Equation (5) provides $S_{i,j}$ values higher than those obtained with the Equation proposed by Dueñas-Osorio and Kwasinski [12].

The two equations have also been compared for other earthquakes than the Tohoku earthquake. In particular, the restoration curves of the infrastructures for the 2010 Chile earthquake [12] have been used for comparison using the restoration curves of Region VIII (which is one of the 15 first-order administrative divisions in Chile). The $S_{i,j}$ index have been plotted in Figure 10, where it appears that the proposed Equation (5) provides higher values of the index with respect to Equation (1) for all the cases analyzed, in particular when there is more than one value of the CCF function over the positive threshold of statistical significance. In conclusion, the same trend observed for the Tohoku earthquake, shown in Figure 3, has been observed in the Chile Earthquake.

7. DECOMPOSITION OF THE RESTORATION CURVES IN INTERVALS RANGING BETWEEN TWO CONSECUTIVE SHOCKS

Careful analysis of the results shown in Figure 3(a) revealed an anomalous behavior of the interdependency index in the Miyagi prefecture, as results indicated a negative value for the combinations power-water and power-gas. This negative value would have implied that power delivery was controlled by water supply and gas delivery. This was not logical, because electricity normally leads in affecting the performance of the other networks (for example, electricity is needed for the operation of pumps and valves, which are themselves essential for the proper functioning of aqueducts and gas pipelines). This incoherent behavior of the interdependency index was also observed in Figure 3(b) for the Iwate prefecture, in which the index of interdependency had a negative value for the combination power-gas.

This anomaly was found with all equations considered, including the one proposed by Dueñas-Osorio and Kwasinski [12], and it was found to be a consequence of the nature of the restoration curves under consideration. The numerical error derives from the data collected after the main shock over a time period during which two strong aftershocks occurred. In fact, these aftershock events have affected the functionality of lifelines, perturbing the restoration curves. The solution to this problem can be found by dividing the data into homogeneous parts of the restoration curves corresponding to the elapsed time between two consecutive strong shocks. Figure 11 shows this operation for the Miyagi region. Figure 11(a) shows the entire data set recorded from the main shock on March 11, 2011, for 47 consecutive days. The vertical dotted lines correspond to the main
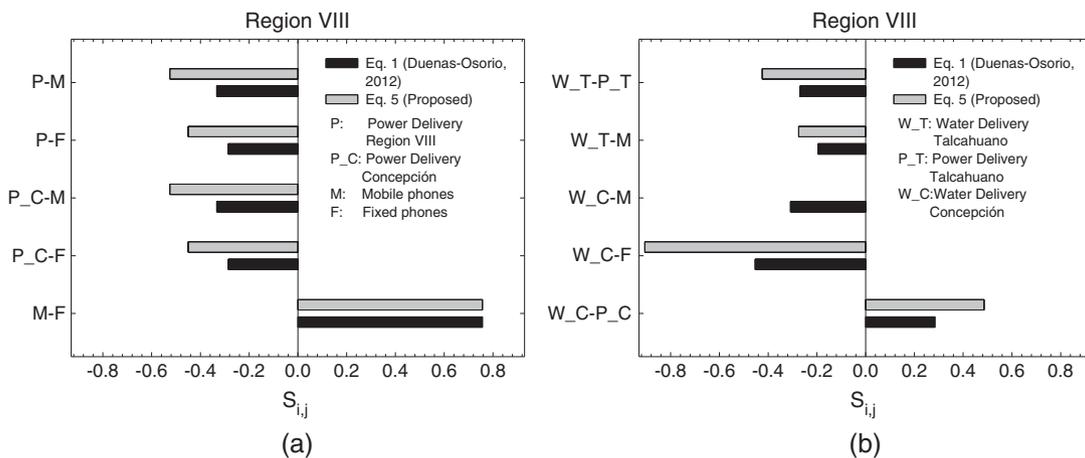
Figure 10. Comparison of different interdependency index (Eqs (1) and Eq. (5)) for region VIII of February 27, 2010 Chile earthquake.
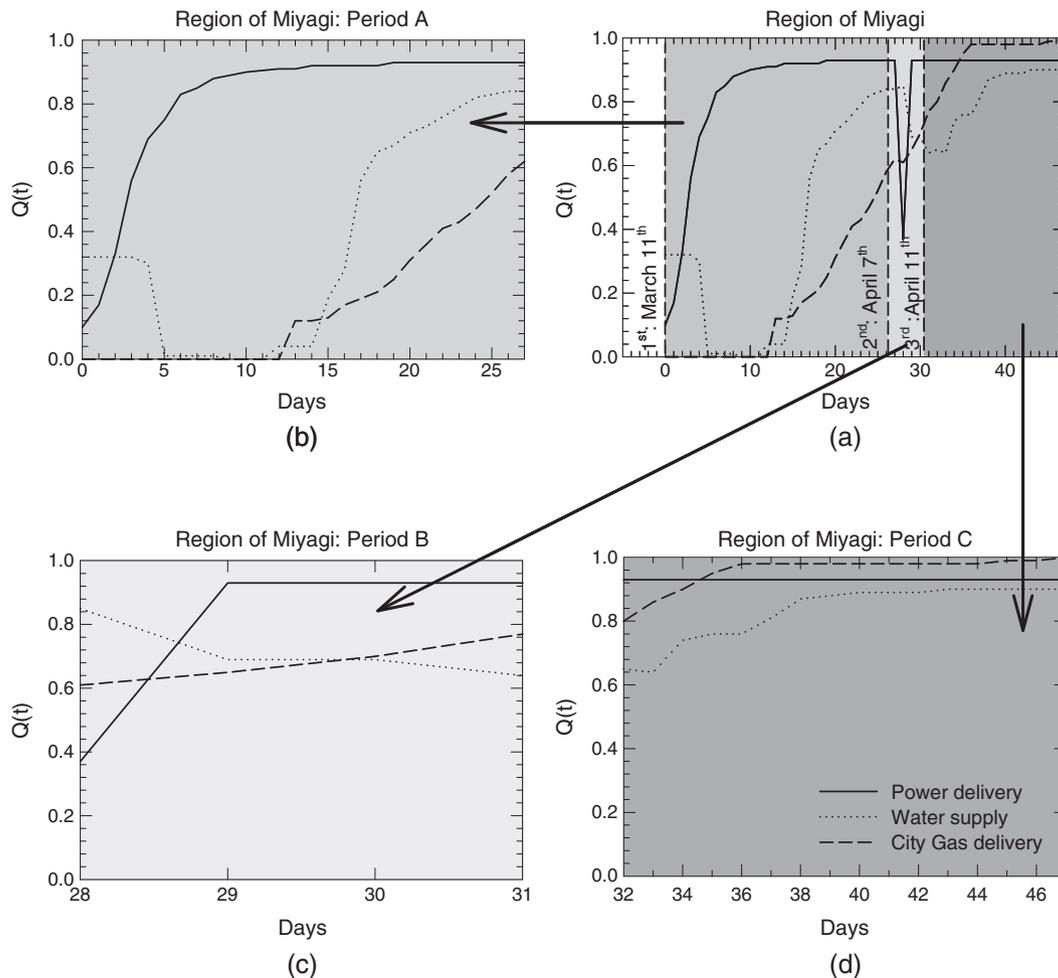
Figure 11. (a) Restoration curves from main shock to the end of the records of data; (b) restoration curves between main shock and first strong aftershock; (c) restoration curves between first strong aftershock and second strong aftershock; (d) restoration curves between second strong aftershock and the end of available records of data.

shocks and aftershocks. Three period ranges are identified: the first from the main shock of March 11 until April 7 when the first main aftershock occurred (Figure 11(b)); the second from April 7 to 11, when the second main aftershock occurred (Figure 11(c)); the third from April 11 to until the end of recorded data (Figure 11(d)). Reanalysis is then performed for each region examined, taking as reference the same periods. For each period, the cross-correlation analysis of the restoration curves is performed after the logarithmic transformation, and the second differences as described earlier.

Figure 12 shows the cross-correlation function for the region of Miyagi calculated over the first period range (period A) of the time series. Looking at the cross-correlation function between power delivery and city gas delivery (Figure 12(b)), it is noted that, now, power delivery leads the city gas delivery restoration process during period A, because there is a high positive value of CCF, over the statistical threshold, at positive lag. This leads to a positive value of the interdependency index, regardless the type of equation used to calculate it. Instead, when the entire time series (47 days) is considered, all the equations used to evaluate the interdependency index give a negative value of $S_{i,j}$ with respect to the cross-correlation between power delivery and city gas delivery. Results from the reanalysis indicate that dividing the time series in intervals between subsequent shocks leads to more logical result compatible with experience-based expectations, because power delivery is now found to lead the restoration process of city gas delivery. Looking at other results, such as the cross-correlation function between water supply and city gas delivery (Figure 12(c)), it is observed that
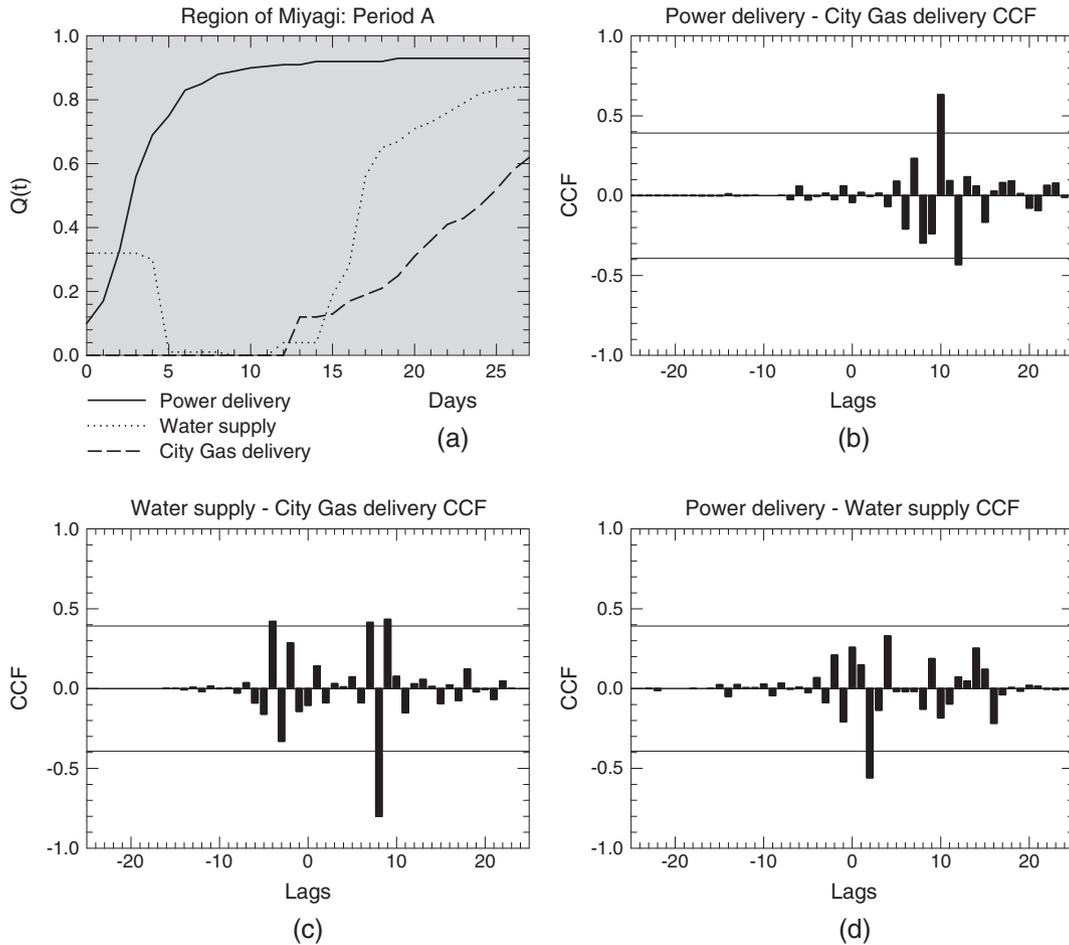
Figure 12. Region of Miyagi: cross-correlation functions for the data of restoration curves from main shock to first strong aftershock.

water supply weakly leads the city gas delivery restoration process during period A. In fact, there are two small positive values of *CCF* above the statistical threshold at positive lags, and only one small positive value of *CCF* above the statistical threshold at negative lag. The results for water supply and city gas delivery obtained in Figure 12(c) for period A of the time series are similar to the results obtained for the entire time series of 47 days shown in Figure 3(a), because the value of the interdependency index is positive for both period ranges. The *CCF* function between power delivery and water supply in Figure 12(d) shows a *weak dependence* of water supply on power delivery, because the largest positive value of the *CCF* function that occurs at positive lag is below the positive threshold of statistical significance, following the definition of weakly dependence provided by Dueñas-Osorio and Kwasinski [12]. Applying Equation (1) [12] to the cross-correlation function in Figure 12(d) related to the first time interval (period A), the value of the interdependency index $S_{i,j}$ is different from zero, because it is using values of the *CCF* function below the threshold of statistical significance. Instead, according to Equation (5), the value of the interdependency index $S_{i,j}$ is equal to 0, because there is no positive value of the *CCF* function above the positive threshold; therefore, the restoration processes of power delivery and water supply are independent. On the other hand, when the second time interval (period B) is considered, the $S_{i,j}$ values do not seem logical, possibly because the time interval considered in that period is too short. To address this issue, it was decided to combine periods B and C. This aggregation is partially justified by the fact that the second aftershock that occurred on April 11 affected only the restoration curves of the prefecture of Fukushima. After this aggregation, by repeating the same procedure, the $S_{i,j}$ values became logical again (results not shown in this article).

Table IV shows the S matrices calculated using Equation (5) for two different time intervals: (i) the maximum duration of the time series (47 days) and (ii) the time interval between the main shock and the first strong aftershock of April 7 (27 days). In gray are highlighted the values of the interdependency indices related to the Power delivery, which switch from negative values to positive values when the analysis time period is reduced from 47 to 27 days. The physical meaning of this variation is that it results in the power network leading the other networks (as mentioned earlier). Furthermore, the $S_{i,j}$ values are shown to become consistent with actual dependencies when considering the time range (27 days) between the main shock and the first strong aftershock, regardless the type of equation used. In fact, the same trend is also observed using Equation (1) [12]. From the aforementioned considerations, it is suggested that the $S_{i,j}$ values should be evaluated using the time interval between the main shock (March 11) and the first strong aftershock (*April 7*). In this way, the

Table IV. Comparison of interdependency index among different time: the values that increase are highlighted in gray.

Region		$S_{i,j}$ 47 days Eq. (5)			$S_{i,j}$ 27 days Eq. (5)		
		Power	Water	City gas	Power	Water	City gas
Miyagi	Power	1.00	−0.35	−0.19	1.00	0.00	0.20
	Water	0.35	1.00	0.31	0.00	1.00	0.31
	City gas	0.19	−0.31	1.00	−0.20	−0.31	1.00
Iwate	Power	1.00	0.55	−0.56	1.00	0.20	0.13
	Water	−0.55	1.00	−0.38	−0.20	1.00	0.51
	City gas	0.56	0.38	1.00	−0.13	−0.51	1.00
Fukushima	Power	1.00	0.47	−0.35	1.00	0.00	0.49
	Water	−0.47	1.00	−0.23	0.00	1.00	−0.27
	City gas	0.35	0.23	1.00	−0.49	0.27	1.00
Yamagata	Power	1.00	0.31	—	1.00	0.35	—
	Water	−0.31	1.00	—	−0.35	1.00	—
Akita	Power	1.00	0.93	—	1.00	0.20	—
	Water	−0.93	1.00	—	−0.20	1.00	—
Ibaraki	Power	1.00	0.20	0.49	1.00	0.20	0.27
	Water	−0.20	1.00	0.87	−0.20	1.00	0.87
	City gas	−0.49	0.87	1.00	−0.27	0.87	1.00
Tochigi	Power	1.00	0.45	—	1.00	0.45	—
	Water	−0.45	1.00	—	−0.45	1.00	—
Aomori	Power	1.00	−0.15	−0.13	1.00	0.42	0.33
	Water	0.15	1.00	0.72	−0.42	1.00	0.80
	City gas	0.13	0.72	1.00	−0.33	0.80	1.00
Chiba	Power	1.00	—	0.23	1.00	—	0.23
	City gas	−0.23	—	1.00	−0.23	—	1.00
Gunma	Power	1.00	0.40	—	1.00	0.40	—
	Water	−0.40	1.00	—	−0.40	1.00	—
Saitama	Power	1.00	0.46	1.00	1.00	0.46	1.00
	Water	−0.46	1.00	−0.46	−0.46	1.00	−0.46
	City gas	1.00	0.46	1.00	1.00	0.46	1.00
Kanagawa	Power	1.00	—	0.55	1.00	—	0.54
	City gas	−0.55	—	1.00	−0.54	—	1.00

perturbation effects of the aftershocks on the restoration curves will be reduced, by focusing only on the perturbation effects of the main shock.

8. CALCULATION OF THE WEIGHT COEFFICIENTS ON THE FIRST PERIOD

In order to evaluate the resilience index given in Equation (10), it necessary to evaluate the weight coefficients (Equation (7)), which depend on the values of interdependency indices. Table V presents a comparison of the weight coefficients obtained using Equation (1) [12] and Equation (5), calculated from the interdependency indices evaluated using the procedure shown in the previous paragraph and the dataset of 27 days (from March 11 to April 7).

Table V. Comparison of weights from Equation (1) and (5): are highlighted in gray the highest values in each region gray the highest values.

Region		w_i from Eq. (1) [12]	w_i from Eq. (5)
Miyagi	Power	0.37	0.34
	Water	0.33	0.37
	City gas	0.30	0.28
Iwate	Power	0.37	0.35
	Water	0.34	0.39
	City gas	0.30	0.26
Fukushima	Power	0.39	0.40
	Water	0.28	0.27
	City gas	0.33	0.34
Yamagata	Power	0.55	0.57
	Water	0.45	0.43
Akita	Power	0.54	0.54
	Water	0.46	0.46
Ibaraki	Power	0.26	0.28
	Water	0.37	0.36
	City gas	0.37	0.36
Tochigi	Power	0.56	0.59
	Water	0.44	0.41
Aomori	Power	0.29	0.33
	Water	0.36	0.34
	City gas	0.36	0.34
Chiba	Power	0.54	0.55
	City gas	0.46	0.45
Gunma	Power	0.56	0.58
	Water	0.44	0.42
Saitama	Power	0.41	0.42
	Water	0.18	0.17
	City gas	0.41	0.42
Kanagawa	Power	0.56	0.61
	City gas	0.44	0.39

8.1. Considerations on the weight coefficients of the power delivery network

The highest weight coefficients calculated using Equation (1) correspond to the power delivery network in all the regions, with the exception of Ibaraki and Aomori. The exception is extended also to the regions of Miyagi and Iwate when Equation (5) is adopted. However, the weight coefficients tend to increase from Equations (1) to (5) in general. It is expected that the lifeline that has the highest weight coefficient in a developed country like Japan should certainly be the power delivery because many infrastructures operate through electric power. Applying Equation (5) leads to an increment of the weight coefficients of the power network in many regions with respect to Equation (1). This may be considered a benefit of the proposed equation. As explained earlier, the only exceptions to this trend were found in the regions of Miyagi and Iwate. Probably the cause of this anomaly in the weight coefficients can be related to the fact that these two regions have common characteristic of the restoration curves that are slower for the prefectures closer to the epicenter.

8.2. Considerations on the weight coefficients of the water network

Other anomalies in the interdependency indices that can be physically justified are in the water distribution network. For example, after the earthquake, the water supply service was interrupted for 2,300,000 households, but because most of the residents in the areas flooded by the tsunami had not returned to live there shortly after the event, most of the damage pipelines remained unrepaired [17]. Therefore, the restoration curves of the water distribution network in these regions was slower (e.g., Miyagi, Iwate, and Fukushima), as shown in Figure 1. As a result of the interdependency analysis, the water distribution network appears to be dependent on the power and gas distribution networks, as shown in Table IV. Furthermore, in the Miyagi Prefecture, the regional water supply system takes water from dams and rivers outside of the Prefecture [13]. Large-diameter welded steel transmission pipelines of these trans-municipal water supply systems suffered major damage, which significantly hindered recovery work during a few weeks [13]. The configurations of these water transmission networks are tree-like structures. Because of poor redundancy of tree networks, the downstream areas of the most upstream location of pipe failures lose water supply. Recovery works of the failed pipes had to be conducted starting from upstream (progressing toward downstream) in order to restore connection between water sources to users. Therefore, remote areas from the water source experienced longer disruption of water service. Results show this dependency of the water networks in the remote areas on the network in the upstream areas.

8.3. Considerations on the weight coefficients of the gas network

Regarding the gas network, the most affected supplier was the Gas Bureau of the City of Sendai [18]. The Minato LNG plant was devastated by the tsunami, which was the main cause of the city gas outage for 359 thousand households (78.2% of the total outage) [13]. Fortunately, the long-distance high-pressure pipeline network transmitting natural gas from the Niigata Prefecture to Sendai performed well. Transmission of natural gas was shut off immediately after the earthquake at the Shiroishi junction valve station [13, 18]. However, after completing safety inspection along the transmission line to Sendai (including 15 valve stations), the network system restarted its operation on March 23, contributing to rapid recovery thereafter [13]. The rapid recovery of the gas distribution network in Miyagi generated a dependency of all the other infrastructures (water and power) on the gas distribution network as shown in Table IV.

9. NUMERICAL RESULTS OF THE REGIONAL RESILIENCE INDEX

The previous section highlighted the importance of properly selecting the data range on which is based the calculation of the interdependency index and, consequently, the calculation of the weight coefficients. It was shown that, when the total time interval includes more than one catastrophic event, the calculation of the index $S_{i,j}$ and, consequently of the weight coefficients, can be problematic, and that better results are obtained when the evaluation is performed only on the first

period interval (between the main shock and the first aftershock) that causes a loss of functionality in at least one of the considered lifelines. Therefore, the weight coefficients of the lifelines calculated for the time series of 27 days (from March 11 to April 7) using Equation (5) were used to calculate the resilience index values using Equation (9) based on four different periods (T_c).

The first period has a length of 1 week (7 days). The second period has a length of 2 weeks (15 days). The third one has a length of 27 days (i.e., the time interval between the main shock and the first aftershock that generates a drop of functionality in at least one lifeline) while the fourth period T_c has a length of 47 days (that is the length of the complete set of data recorded after the main shock). These different values of T_c were assumed to evaluate the value of the index of resilience at different intervals. A resilience index evaluated a week after the main shock gives information about the extent of the damage suffered by the physical infrastructure in a region and can give information about the vulnerability of a region and its ability to restore services to the previous condition for a hazard of given magnitude. The resilience index is mainly influenced by physical and geographical

Table VI. Regional Resilience with Eq. (5): are highlighted in gray the maxima and minima values within each time interval.

Region	Infrastructure	T_w	w_i	R_{tot} 7 days	R_{tot} 15 days	R_{tot} 27 days	R_{tot} 47 days
Miyagi	Power Water City gas	07 Apr.	0.34 0.37 0.28	0.26	0.30	0.46	0.63
Iwate	Power Water City gas	07 Apr.	0.35 0.39 0.26	0.36	0.45	0.53	0.66
Fukushima	Power Water City gas	07 Apr.	0.40 0.27 0.34	0.45	0.55	0.66	0.76
Yamagata	Power Water	07 Apr.	0.57 0.43	0.67	0.83	0.90	0.93
Akita	Power Water	07 Apr.	0.54 0.46	0.86	0.91	0.95	0.95
Ibaraki	Power Water City gas	07 Apr.	0.28 0.36 0.36	0.44	0.67	0.80	0.88
Tochigi	Power Water	07 Apr.	0.59 0.41	0.69	0.84	0.91	0.94
Aomori	Power Water City gas	07 Apr.	0.33 0.34 0.34	0.65	0.83	0.90	0.93
Chiba	Power City gas	07 Apr.	0.55 0.45	0.64	0.70	0.83	0.90
Gunma	Power Water	07 Apr.	0.58 0.42	0.72	0.86	0.92	0.95
Saitama	Power Water City gas	07 Apr.	0.42 0.17 0.42	0.82	0.91	0.95	0.97
Kanagawa	Power City gas	07 Apr.	0.61 0.39	0.85	0.93	0.96	0.98

interdependencies. The lifeline interdependencies or the proximity to the epicenter of the earthquake as well as the proximity of a region to the East coast are the predominant factors in the short time interval. The resources available for the reconstruction have minor importance at this stage, while they become
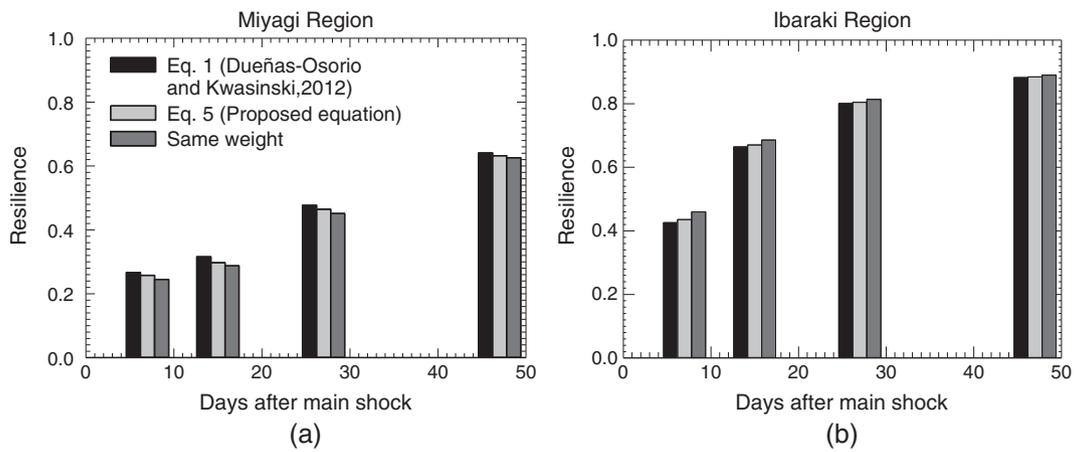
Figure 13. Comparison between the new regional resilience indices obtained using three types of weight coefficients for the regions of (a) Miyagi and (b) Ibaraki.
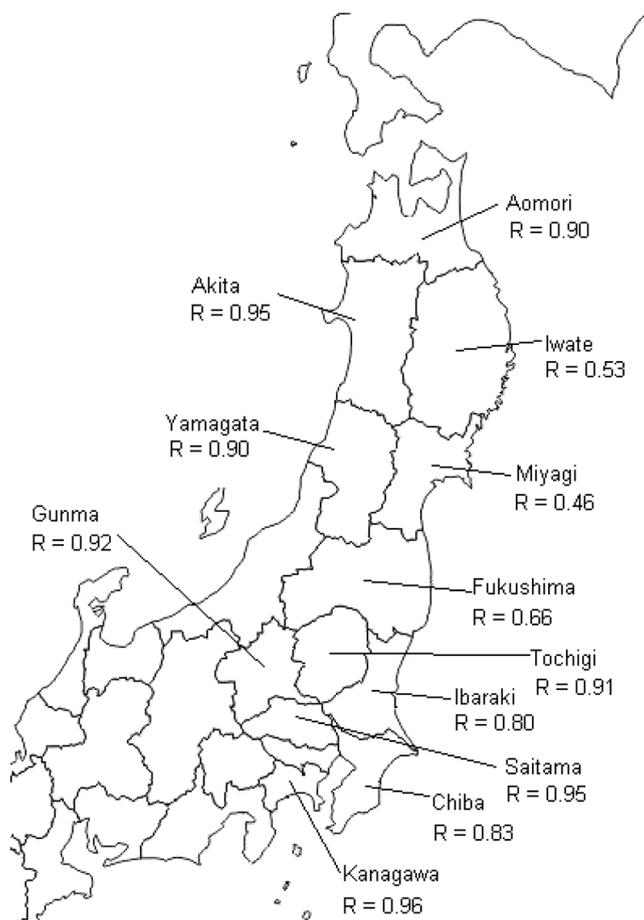
Figure 14. Regional resilience 27 days after the main shock evaluated using Equation (5) to evaluate the weight coefficients.

more important as time goes on. Resilience indices are shown in Table VI, with the maximum and minimum values within each time interval highlighted in gray. Analyzing the results in Table VI, it is observed that for the time intervals equal to 15, 27, and 47 days, the region closest to the epicenter (Miyagi) and the one farthest from the epicenter (Kanagawa) have, respectively, the lowest and the highest value of resilience. The only exception for the period of 7 days is the Akita region, which is the one shown to have the highest resilience index even though it is not the region farthest from the epicenter. This anomaly can be explained by the fact that the Akita region, although not far from the epicenter of the earthquake, is on the west coast, and that this coast of Japan did not suffer damage from the tsunami that devastated the East Coast of Japan after the main shock.

Figure 13 shows a comparison of the resilience index for the Miyagi prefecture for the different chosen time ranges, calculated using the weights obtained by the interdependency index of Equation (1) [12] and Equation (5). For comparison, the value of the resilience index obtained using the same weights for each lifeline is shown in that figure. It can be observed that the three values that change in time are not so different (Figure 13). This implies that the weight coefficients do not influence the results significantly. It would be less computationally demanding to assign the same weight to all the infrastructures to obtain a value of the regional resilience index. However, the methodology presented in this article provides a mathematical approach to the problem, by creating a rational procedure to evaluate the weight coefficients. Furthermore, the methodology presented is also useful to identify the most important lifelines, which correspond to the ones with the highest value of the weight coefficients in the region. Finally, analysis results here may have been influenced by the fact the restoration curves were available for only three types of lifelines. Probably, by increasing the number of lifelines in the analysis, the resilience index could have been found to be more sensitive to the weight coefficients. Finally, Figure 14 geographically displays the regional resilience indices for all the regions affected by the earthquake, as calculated using the procedure described earlier.

10. REMARKS AND CONCLUSIONS

A methodology has been proposed for the calculation of regional resilience index starting from the values of resilience for individual infrastructures. The resilience index of each infrastructure is evaluated with Equation (9) proposed by Cimellaro *et al.* [2, 15, 16] using restoration curves data from the 2011 Tohoku earthquake in Japan. The resilience indices of the individual lifelines are then combined using weight coefficients, which are calculated on the basis of a matrix of interdependency $S_{i,j}$ calculated for each region. Once the weight coefficients are known, the regional resilience index is evaluated, multiplying the resilience of each lifeline by the corresponding weight coefficient and adding the results obtained for all regions. A detailed analysis of the interdependency index has been performed, and a new equation that improves the one proposed by Dueñas-Osorio and Kwasinski [12] has been presented. The proposed equation takes into account the level of statistical significance for each *CCF* function, considering only the values above the statistical threshold. More importance has been given to the peak values and to the number of times in which the *CCF* function exceeds the threshold of statistical significance. Although it was observed for this particular example that the weight coefficients did not significantly influence the value of the resilience index, the methodology presented in this article provides a mathematical approach to the problem, by creating a rational methodology to select the weight coefficients.

Furthermore, based on the result of this case study, it is suggested to use the period range between the main shock and the first aftershock for the evaluation of the weight coefficients. More infrastructure disruption data (from this and other earthquakes) would be needed to generalize this finding, but such data is scarce and difficult to obtain, being usually own by private companies or public organizations that are protective of this data. However, it is reasonable to expect that aftershocks can affect the restoration process and modify the restoration curve. Future data will allow to quantify changes in the restoration curves as a function of *magnitude* of the shocks and *distance from the epicenter*, as well as the intrinsic properties of the physical infrastructures affected by the earthquake. However, whether or not the aftershocks are going to affect the shape of the restoration curves, the results presented here indicate that a good way to obtain meaningful result is to consider the time range

between the two perturbations. Understandably, these two perturbations cannot be too close; otherwise, the number of data points between the two events will not be enough to estimate the correlation coefficients of the two series.

Finally, it is recognized that the results presented in this paper may have been influenced by the fact that only the restoration curves of three lifelines have been considered. Future research may focus on testing the proposed methodology for the calculation of the regional resilience index using a higher number of restoration curves and earthquake data sets.

REFERENCES

 1. Cimellaro GP, Reinhorn AM, Bruneau M. Framework for analytical quantification of disaster resilience. *Engineering Structures* 2010; **32**(11):3639–3649.
 2. Cimellaro GP. Computational framework for resilience-based design (RBD) CH11. In *Handbook of seismic risk analysis and management of civil infrastructure systems*, Tesfamariam S, Goda K (eds). Woodhead Publishing Limited: 80 High Street, Sawston, Cambridge, CB22 3HJ, UK, 2013; 810.
 3. Arcidiacono V, Cimellaro GP, Reinhorn AM, Bruneau M. Community resilience evaluation including interdependencies. *15th World Conference on Earthquake Engineering (15WCEE)*, Lisbon, Portugal, September 24–28, 2012.
 4. Rinaldi SA, Peerenboom JP, Kelly TK. Identifying, understanding, and analyzing critical infrastructure interdependencies. *IEEE Control Systems Magazine* 2001; **21**(6):11–25.
 5. Paton D, Johnston D. *Disaster Resilience an Integrated Approach*. Charles C Thomas Publisher Ltd.: Springfield, Illinois, USA, 2006.
 6. Bigger JE, Willingham MG, Krimgold F, Mili L. Consequences of critical infrastructure interdependencies: Lessons from the 2004 hurricane season in Florida. *International Journal of Critical Infrastructures* 2009; **5**(3):199–219.
 7. Delamare S, Diallo AA, Chaudet C. High-level modelling of critical infrastructures' interdependencies. *International Journal of Critical Infrastructures* 2009; **5**(1-2):100–119.
 8. Kakderi K, Argyroudis S, Pitilakis K. State-of-the-art literature review of methodologies to assess the vulnerability of a "system of systems". *D2.9*, Aristotle University of Thessaloniki, 2011.
 9. Kongar I, Rossetto T. A framework to assess the impact of seismic shocks on complex urban critical infrastructure networks. *15th World Conference on Earthquake Engineering (15WCEE)*, Lisbon, Portugal, September 24–28, 2012.
10. Kjolle GH, Utne IB, Gjerde O Risk analysis of critical infrastructures emphasizing electricity supply and interdependencies. *Reliability Engineering & System Safety* 2012; **105**:80–89.
11. Poljanšek K, Bono F, Gutiérrez E seismic risk assessment of interdependent critical infrastructure systems: the case of European gas and electricity networks. *Earthquake Engineering and Structural Dynamics* 2012; **41**(1):61–79.
12. Duenas-Osorio L, Kwasinski A. Quantification of Lifeline System Interdependencies after the 27 February 2010 M-w 8.8 Offshore Manic, Chile, Earthquake. *Earthquake Spectra* 2012; **28**:S581–S603.
13. Nojima N. Restoration Processes of Utility Lifelines in the Great East Japan Earthquake Disaster, 2011. *15th World Conference on Earthquake Engineering (15WCEE)*, Lisbon, Portugal, September 24–28, 2012.
14. Shumway RH, Stoffer DS. *Time Series Analysis and Its Applications*. Springer: New York, 2006.
15. Cimellaro GP, Reinhorn AM, Bruneau M Seismic resilience of a hospital system. *Structure and Infrastructure Engineering* 2010; **6**(1-2):127–144.
16. Cimellaro GP, Villa O, Bruneau M. Resilience-based design of natural gas distribution networks. *ASCE Journal of Infrastructure Systems* 2013. DOI: 10.1061/(ASCE)IS.1943-555X.0000204
17. Miyajima M. Damage Analysis of Water Supply Facilities in the 2011 Great East Japan Earthquake and Tsunami. *15th World Conference on Earthquake Engineering (15WCEE)*, Lisbon, Portugal, September 24–28, 2012.
18. Mori S, Chiba K, Koike T. Seismic Performance Analysis of the Transmission Gas Pipeline in the 2011 Great East Japan Earthquake. *15th World Conference on Earthquake Engineering (15WCEE)*, Lisbon, Portugal, September 24–28, 2012.